Hydrogeology Journal (2020) 28:853–868
https://doi.org/10.1007/s10040-020-02109-x

REPORT

Rapid groundwater recharge dynamics determined from hydrogeochemical and isotope data in a small permafrost watershed near Umiujaq (Nunavik, Canada)

M. Cochand[1,2] · J. Molson[1,2] · J. A. C. Barth[3] · R. van Geldern[3] · J.-M. Lemieux[1,2] · R. Fortier[1,2] · R. Therrien[1,2]

Received: 2 October 2018 / Accepted: 1 January 2020 / Published online: 25 January 2020

Abstract

Hydrogeochemical data are used to better understand recharge dynamics and to support a hydrogeological conceptual model in a 2-km^2 watershed in a discontinuous permafrost zone in Nunavik, Canada. The watershed contains an upper (surficial) and lower aquifer within Quaternary deposits, above and below a marine silt layer containing ice-rich permafrost mounds. The analysis is based on water samples from precipitation, groundwater monitoring wells, ground ice in permafrost mounds, thermokarst lakes and a perennial stream. Groundwater geochemistry in both aquifers reflects young, poorly evolved waters, with mainly Ca-HCO_3 water types and low mineralisation ranging from 11 to 158 mg/L total dissolved solids (TDS), implying short pathways and rapid travel times of a year or less. While relatively low, TDS signatures in groundwater and surface water show increasing values downgradient. Groundwater isotope values ($\delta^{18}O_{H2O}$ and $\delta^{2}H_{H2O}$) are often strongly influenced by snowmelt, while those of thermokarst lakes show evidence of evaporation. Recharge along the cuesta contributes to a transverse component of groundwater flow within the valley with higher TDS and $\delta^{13}C_{DIC}$ values influenced by open-system weathering. Even where permafrost-free, the marine silt unit has a strong confining effect and plays a more important role on recharge dynamics than the discontinuous permafrost. Nevertheless, the vulnerability of these types of hydrogeological aquifer systems is expected to increase due to rapid recharge dynamics associated with the gradual loss of the confining effect of permafrost. This hydrogeochemical data set will be useful as a baseline to document impacts of permafrost degradation on the hydrogeological system.

Keywords Hydrochemistry · Cold regions hydrogeology · Natural isotope tracers · Permafrost · Canada

Introduction

The impacts of climate change have been significant in northern environments. Increases in air temperature, for example, have already resulted in extensive permafrost degradation on a global scale (Grosse et al. 2011; Romanovsky et al. 2010), affecting northern ecosystems, landscapes, ground stability and infrastructure, as well as indigenous populations and their way of life (Ford 2009; Kokelj and Jorgenson 2013; Rowland and Coon 2016). Moreover, permafrost degradation will likely continue over the coming decades. Future climate change simulations, for example, have predicted that the global permafrost surface area will decrease between 37 and 81% by the end of this century (Stocker 2014).

In addition to the impacts of climate change, northern communities in Nunavik, Canada, and elsewhere in arctic and subarctic areas, also face another challenge: ensuring good quality drinking water for sustainable growth and economic development (Messier et al. 2007). In this perspective, groundwater may become a potential resource as water trapped in permafrost ice will be released and may become available for pumping. Furthermore, the loss of frozen confining layers will likely increase groundwater recharge (Lemieux et al. 2016). However, the impact of permafrost degradation

This article is part of the topical collection "Hydrogeology of a cold-region watershed near Umiujaq (Nunavik, Canada)"

✉ J. Molson
John.Molson@ggl.ulaval.ca

[1] Département de Géologie et de Génie Géologique, Université Laval, 1065 avenue de la Médecine, Québec, Québec G1V 0A6, Canada

[2] Centre d'études nordiques, Université Laval, 2405 rue de la Terrasse, Québec, Québec G1V 0A6, Canada

[3] Department Geographie und Geowissenschaften, GeoZentrum Nordbayern, Friedrich-Alexander-Universität Erlangen-Nürnberg, Erlangen, Germany

on groundwater quality and availability is still poorly documented (Cochand et al. 2019).

The impacts of permafrost degradation on the hydrosphere will be significant, particularly on river baseflow and groundwater flow systems (Bense et al. 2009; Boucher and Carey 2010; Carey et al. 2013; McKenzie and Voss 2013; Walvoord and Kurylyk 2016; Walvoord et al. 2012; Woo et al. 2008; Ye et al. 2009). However, most impact studies have focused only on surface water, while only a few have considered groundwater flow systems and even fewer have included groundwater geochemistry, mostly due to the high costs and challenges of accessing northern groundwater research sites (Cochand et al. 2019). Most groundwater studies in permafrost environments have therefore relied either on numerical modelling (Bense et al. 2009; Bosson et al. 2013; Evans and Ge 2017; Frampton et al. 2013; Kurylyk et al. 2016; McKenzie and Voss 2013; Walvoord et al. 2012; Wellman et al. 2013; Woo et al. 2008), or on indirect groundwater monitoring such as river base flow, springs, icings and mine infiltration waters (Callegary et al. 2013; Carey et al. 2013; Clark and Lauriol 1997; Clark et al. 2001; Douglas et al. 2013; Michel 1986; Utting et al. 2013). While discontinuous permafrost is more sensitive to climate warming and will degrade more rapidly than continuous permafrost (Douglas et al. 2013), only a few studies have directly investigated groundwater via wells or piezometers, most of which are located in the continuous permafrost zone (Alexeev and Alexeeva 2003; Cheng and Jin 2013; Claesson Liljedahl et al. 2016; Ma et al. 2017; Stotler et al. 2011, 2009). These previous studies have shown that geology, residence time and permafrost coverage can have significant effects on groundwater hydrogeochemistry.

In this context, the interpretation of various natural groundwater tracers including major ions, dissolved inorganic and organic carbon (DIC, DOC, and their stable and radio isotopes), as well as noble gases, can provide valuable information on groundwater recharge dynamics, flow paths and residence times in degrading permafrost environments (Callegary et al. 2013; Lacelle and Vasil'chuk 2013; Utting et al. 2013).

Based on a groundwater monitoring network installed in collaboration with the Quebec Ministry of Environment (Fortier et al. 2017), this study aims to explore how natural groundwater tracers can help infer groundwater flow and recharge behavior in a small watershed within the discontinuous permafrost zone in Nunavik, Quebec, Canada. This study will also support the development of a conceptual model for groundwater flow in the complex multi-layer aquifer system of the watershed (Lemieux et al. 2020, this issue). Surface water, shallow and deep groundwater, as well as ground ice in permafrost mounds, are investigated to show how these compartments are connected and how they may be affected by climate warming. Finally, these results are used to evaluate if groundwater, in similar hydrogeological contexts, could become a suitable resource for high-quality drinking water in northern communities.

Study area

The study area is a 2 km^2 watershed (Fig. 1) located in the Tasiapik Valley, close to the Inuit community of Umiujaq (Inuktitut: ᐅᒥᐊᔪᖅ, Nunavik, Canada) along the eastern shore of Hudson Bay (56°33′ N, 76°31′ W). The site lies at the margin between shrub tundra (birch, willow and alder) and forest tundra (black spruce, *Picea mariana*) with lichens covering the topographical highs (Provencher-Nolet 2014; Truchon-Savard and Payette 2012). All vegetation is composed of C3-type plants. The climate is subarctic and the annual mean air temperature between 2013 and 2017 was −1.6 °C (Lemieux et al. 2016). The total annual precipitation over the same period was approximately 645 mm, of which about 50% falls as snow (Lemieux et al. 2020, this issue).

The impacts of climate change can already be observed in Nunavik as mean annual air temperatures have increased by about 2–3 °C since the mid-1990s compared with the 1961–1990 reference period (Lemieux et al. 2016). Projections for Nunavik from the Canadian Regional Climate model (CRCM) indicate that, by 2050, the mean annual temperature will increase by 3 °C in winter and 1.5 °C in summer, and that annual precipitation will increase by 25% (Brown et al. 2012).

The watershed is in a discontinuous permafrost zone, with permafrost located in mounds formed within a marine silt unit (see next section). After the retreat of the Tyrrell Sea between 7,000 and 2,000 years BP, this silt unit was exposed to cold temperatures, which led to aggradation of ice-rich permafrost (Fortier et al. 2020, this issue). Previous studies have shown that permafrost in the watershed is currently degrading due to climate warming (Beck et al. 2015; Chouinard et al. 2007; Fortier and Aubé-Maurice 2008).

To investigate the impact of climate change on groundwater in northern regions, the *Immatsiak* monitoring network was installed in the watershed, as part of the Quebec provincial groundwater monitoring network (RSESQ). The *Immatsiak* network consists of nine groundwater wells and three ground-temperature monitoring boreholes distributed over seven stations (Fortier et al. 2017; Lemieux et al. 2016). Four shallow groundwater piezometers and a stream-flow gauging station have also been installed at the watershed outlet (Fig. 1).

The geology in the watershed consists of Quaternary deposits overlying bedrock. A three-dimensional (3D) cryo-hydrogeological model of the Quaternary deposits has been developed based on geophysical surveys (Banville 2016), geological mapping, and borehole logs (Fortier et al. 2020, this issue). A 3D perspective of the model, including vertical cross-sections which illustrate the distribution of the cryo-

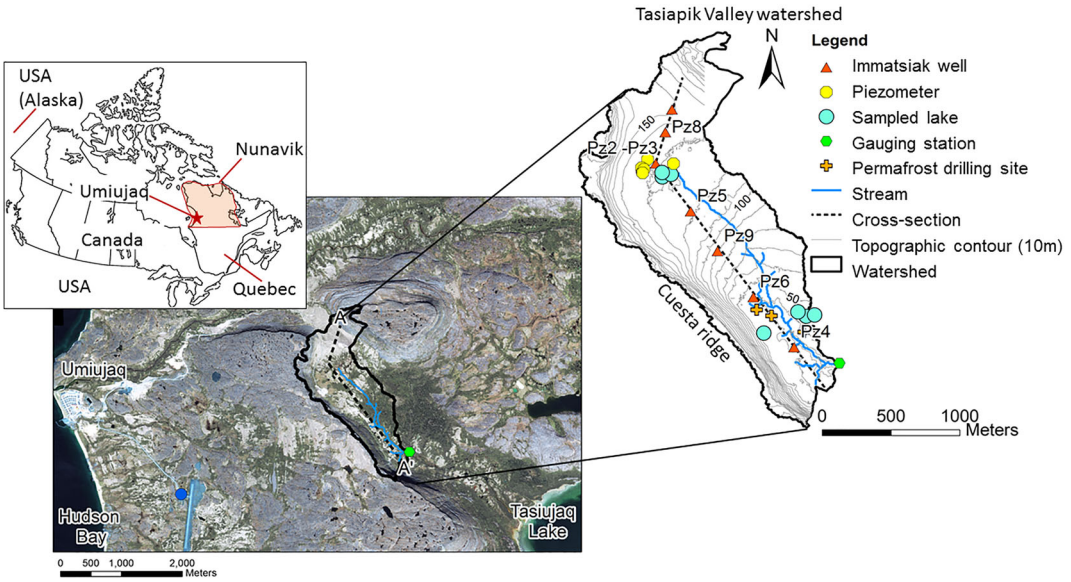

Fig. 1 Location of the study site close to the Inuit community of Umiujaq, Nunavik, Canada

hydrogeological units, is shown in Fig. 2. From bottom to top, the Quaternary deposits are composed of frontal moraine deposits (gravel, pebble and stone, GxT), fluvioglacial sediments (sand and gravel, Gs), marine silts (Ma) that contain the permafrost mounds, and intertidal (Mi) and littoral sands (Mb). These Quaternary deposits are underlain by bedrock consisting of basalts (Ri) and quartz arenite (Rs) (Fig. 2). Further details on the Quaternary geology can be found in Fortier et al. (2020, this issue), Lemieux et al. (2016), and Banville (2016).

The watershed is bounded to the west by the cuesta cliffs (Fortier et al. 2020, this issue) and to the east by the Umiujaq Hill. Two aquifers have been identified within the watershed (Fig. 2). A thin surficial aquifer, in the upper part of the Quaternary sequence, is located in sands (Mi and Mb formations) and is underlain by marine silts (Ma formation). The extent of this aquifer is limited to the upper part of the valley, lying approximately between groundwater monitoring wells Pz8 and Pz9 (Fig. 2). At well Pz2, this surficial aquifer is 4.5 m thick. A deeper aquifer is located in sand and gravels (GxT and Gs formations), below the marine silt unit. This aquifer is unconfined in the upper part of the watershed between wells Pz1–Pz8 (Fig. 1). In the lower part of the watershed, the aquifer is confined by the overlying marine silt unit and the permafrost mounds (Fig. 2). The thickness of the lower aquifer varies between 5 and 30 m—Fig. 2; see also Fortier et al. (2020, this issue). The marine silt unit (Ma), which varies in thickness from 0 to 30 m, also acts as a

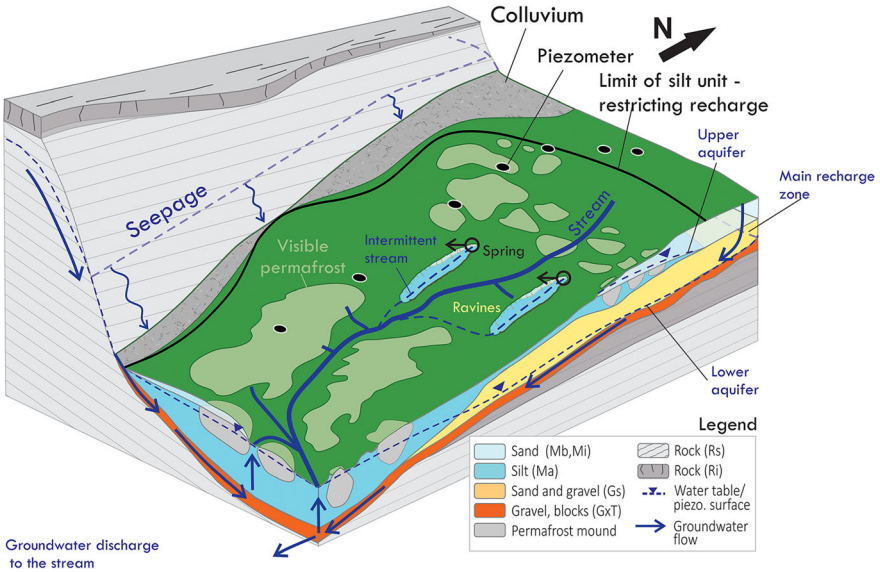

Fig. 2 Perspective 3D conceptual model of the cryo-hydrogeological system within the watershed (from Lemieux et al. 2020, this issue)

confining layer between the upper and lower aquifers in the upper part of the watershed downstream of well Pz8 (Lemieux et al. 2016). A perennial stream drains the watershed in the lower part of the watershed towards Tasiujaq Lake (Lemieux et al. 2020, this issue), while thermokarst lakes are present throughout the watershed, providing evidence of permafrost degradation (Beck et al. 2015).

Water infiltrating in the upper (northern) part and in the western portion of the watershed (through the highly fractured cuesta ridge) recharges the lower aquifer through deep percolation (Fig. 2; see also Lemieux et al. 2020, this issue). However, for the remaining part of the watershed where the silt layer confines the lower aquifer, the infiltrating water either recharges the surficial aquifer or flows directly to the stream through surface runoff. Moreover, the thick unsaturated zone beneath the silt layer in the upper part of the valley (Fig. 2) likely acts as a capillary barrier preventing vertical drainage of the surficial aquifer. Groundwater in the lower aquifer below the silt layer leaves the watershed under confined conditions. Artesian conditions in the lower aquifer were observed at well Pz4 during winter, indicating vertical upward flow toward the stream in this area. A detailed analysis of the stream and piezometer hydrographs shows that the lower aquifer significantly contributes to stream baseflow in winter, but much less in summer— see Lemieux et al. (2020, this issue) for a detailed water budget and the seasonal variation of groundwater levels.

Materials and methods

Sampling campaign

Four summer field campaigns were conducted at the Umiujaq research site between 2013 and 2016, usually between the end of June and the middle of July. Water samples were taken from precipitation, from groundwater in the upper and lower aquifers, from the stream and lakes, as well as from ground ice in several permafrost mounds. Groundwater samples were analysed for natural tracers including major ions (Ca^{2+}, Mg^{2+}, K^{+}, Na^{+}, total alkalinity, Br^{-}, Cl^{-}, F^{-}, NO_3^{-}, NO_2^{-} and SO_4^{2-}), nutrients (NH_4^{+} and total inorganic P), trace elements (Al, Sb, Ag, As, Ba, Be, Bi, B, Cd, Cr, Co, Cu, Sn, Fe, Li, Mn, Mo, Ni, Pb, Se, Si, Sr, Ti, U, V and Zn), water stable isotopes (expressed as $\delta^{18}O_{H2O}$ and $\delta^{2}H_{H2O}$), dissolved carbon phases (DIC and DOC) and their stable isotope ratios ($\delta^{13}C_{DIC,DOC}$), as well as $^{3}H/^{3}He$ (tritium/helium ratios) for age dating. Surface-water samples were analysed for major ions, nutrients, trace elements, water stable isotopes as well as carbon phases and their stable isotopes. Precipitation and ground ice were analysed for water stable isotopes. Physico-chemical parameters including pH, electrical conductivity (EC), water temperature, dissolved oxygen (DO) and redox potential (ORP) were measured in the field using a multi-parameter probe (YSI Pro Plus). Duplicates and field blanks, respectively 10 and 1% of the samples, were taken to verify procedure quality.

Samples were collected following standard protocols (Blanchette et al. 2010). Major ions, nutrients, trace elements, DIC and DOC were filtered at 0.45 μm. In addition, major cations and trace elements were acidified using HNO_3^{-}. Nutrients were acidified using H_2SO_4, while DIC and DOC samples were preserved using 20 μL of a concentrated $HgCl_2$ solution. Samples for major ions, nutrients, trace elements and water stable isotopes were stored in polyethylene vials, while DIC and DOC samples were stored in US Environmental Protection Agency (EPA) amber glass vials. Vials free of preservative agents were rinsed three times with the sampled water before sample collection. Vials containing preservative agent were filled to the brim without overflowing. All vials were carefully closed and secured using Parafilm and stored at 4 °C until analysed.

Precipitation samples were collected monthly at the Umiujaq airport with a rain sampler (Palmex RS1; Michelsen et al. 2018) to establish the local meteoric water line (LMWL) for water isotopes. In addition, during the 2015 and 2016 field campaigns, event-driven sampling of precipitation for major ions and water isotopes was conducted within the watershed using a buried HDPE bottle connected to the surface via a funnel and tubing located close to well Pz2 (Fig. 1).

Groundwater from the surficial aquifer (Fig. 2) was sampled at well Pz2 and at four piezometers (Pz1405, Pz1404b, Pz1402 and PzDP), while groundwater from the lower aquifer was sampled at wells Pz3, Pz4, Pz5, Pz6, Pz8 and Pz9. Groundwater sampling was based on a minimal drawdown (low flow) procedure (Puls and Barcelona 1996) using a bladder pump (Solinst model 407 SS). Drawdown was monitored during purging and sampling to ensure that it did not exceed 10 cm. Purging was considered complete when the primary physico-chemical parameters (pH, EC, temperature, DO and ORP) had stabilised for at least three measurements, which were taken every 5 min. Stabilisation criteria were set to ±0.2 for pH, ±0.2 °C for temperature, ±4% for EC, ±20 mv for ORP, and ±0.4 mg/L for DO (Blanchette et al. 2010).

Stream water was sampled every year at the gauging station (at the outlet of the watershed) for major ions, nutrients, trace elements, water isotopes, as well as for DIC, DOC and their $\delta^{13}C$ isotope ratios.

During the 2016 sampling campaign, a more detailed study of the upstream part of the stream was also completed. In order to monitor groundwater exfiltration, samples and physico-chemical parameters were recorded at 25 points along the stream, extending 1.9 km upstream of the gauging station. All physico-chemical parameters and samples were collected in the middle of the stream. To highlight changes in discharge

along the stream, several stream gauging measurements were carried out on July 10, 2016 using the salt dilution slug-injection method (Moore 2004).

Among the many small lakes and ponds found within the studied watershed, 16 were sampled for water isotopes. Physico-chemical parameters and samples were collected 1 m from the shore in the middle of the water column.

In order to measure water isotopes of ground ice in the permafrost mounds, a STIHL 08 S gasoline-powered auger (Calmels et al. 2005) was used to drill to a depth of 5 m within three ice-rich permafrost mounds (Fig. 1). At the three drilling sites, ground ice samples were taken every 0.10–0.25 m depending on the drilling conditions, core recovery and ice content. Representative samples were thus obtained from the first 5 m of permafrost. To prevent contamination of the isotope ratios in the permafrost core, drilling was performed without any water or other drilling fluid. Samples were carefully wrapped in airtight plastic bags and stored in a portable freezer for transport to the laboratory where they were stored in a chest freezer. Core surfaces were scraped clean to avoid contamination and then melted in airtight boxes. Melted water was then sampled for water stable isotopes.

Tracers for groundwater dating were also sampled in wells Pz2, Pz4, Pz6, Pz8, and Pz9 (Fig. 1). $^{3}H/^{3}He$ samples were collected during field campaigns in 2013 and 2015 using 1,000-ml HDPE bottles for ^{3}H and diffusion samplers for ^{3}He. Concentrations of pCO_2 in water were calculated using PHREEQC (Parkhurst and Appelo 2014), based on alkalinity, temperature, and pH.

Hydrogeochemical analysis and data quality

Major ions, nutrients, and trace elements were analysed at Maxxam Analytics Inc. in Quebec City. Water stable isotopes, as well as carbon phases and carbon isotopes were sent to a laboratory at the Geozentrum Nordbayern at the Friedrich-Alexander-Universität Erlangen-Nürnberg (Erlangen, Germany) for analysis. Water stable isotopes were analysed for $\delta^{18}O_{H2O}$ and $\delta^{2}H_{H2O}$ by an isotope ratio infrared spectroscopy analyzer (L 1102/ICRDS, Picarro Inc., Santa Clara, CA, USA). Raw data and sample-to-sample memory as well as instrument drift were corrected according to van Geldern and Barth (2012). Results are presented herein as δ-values relative to the Vienna Standard Mean Ocean Water (VSMOW) in per mil (‰). The sample standard deviations (1σ) were less than 0.1 and 1.0‰ for $\delta^{18}O_{H2O}$ and $\delta^{2}H_{H2O}$, respectively.

DIC and DOC and their $\delta^{13}C$ ratios were analysed with a OI Analytical Aurora 1030 W TIC-TOC analyzer (OI Analytical, College Station, Texas) coupled to a Thermo Scientific Delta V Plus isotope ratio mass spectrometer (IRMS; Thermo Fisher Scientific, Bremen, Germany). The standard deviations for the DIC and DOC concentration measurements were each less than 0.03 mmol/L, while the 1σ precision of the DIC and DOC isotope measurements was better than 0.3‰. Details of coupling the OI analyzer to the IRMS are described in St-Jean (2003) and van Geldern et al. (2013). $\delta^{13}C_{DIC,\ DOC}$ ratios are presented herein as δ-values relative to Vienna Pee Dee Belemnite (VPDB) in ‰.

$^{3}H/^{3}He$ samples were sent to the Noble Gas Lab at the University of Utah (Salt Lake City, USA) for analysis. The measurements were made by helium ingrowth and analysed by a Mass Analyzers Products – Model 215–50 Magnetic Sector Mass Spectrometer; uncertainty on ^{3}H was ±0.3 TU.

Duplicates and blanks showed no major variations or signs of contamination. The quality of the major ion analysis was verified with ionic balances (Hounslow 1995). Due to the low concentrations of dissolved solids, an error in the ionic balance of less than 10% was considered acceptable. Five samples with an error over 10% were discarded (Hounslow 1995) and not included in the remainder of the study. Samples from wells Pz3 and Pz5 were also discarded as these wells did not seem connected to the groundwater flow system.

Results

Major ions

Graphical representation and interpretation of major ions are based on Piper and Stiff diagrams (Piper 1944; Stiff 1951). Major ion hydrochemistry is particularly helpful to distinguish the different water types present within a watershed (Back 1966).

Results of the major ion hydrochemistry are presented in Table 1. All samples from the lower aquifer have a Ca-HCO_3 water type with total dissolved solids (TDS) concentrations ranging from 66 to 158 mg/L. Stream water samples also present a Ca-HCO_3 water type, with TDS concentrations increasing from 20 to 96 mg/L, increasing from upstream to downstream.

Water samples from the upper surficial aquifer have relatively lower mineralisation (11–54 mg/L TDS) and show water-types varying from Ca-HCO_3 (four samples), Na-HCO_3 (four samples), Ca-Cl (two samples) and Na-Cl (two samples). The hydrogeochemical signatures of the stream water, deeper groundwater, and surficial groundwater are shown in the Piper diagram of Fig. 3a. The Piper diagram suggests that groundwater in the lower aquifer can be divided into two groups. The first group corresponds to upstream wells Pz8, Pz9, Pz6, which plot together in the Ca-HCO_3 area, while the second group is for downstream well Pz4, which plots in the same area as stream water with generally higher SO_4^{2-} and

Table 1 Summary of the hydrogeochemical data from collected groundwater (GW) and surface water samples

Location	Date	pH	EC	Temp	Depth to GW	TDS	Ca^{2+}	Mg^{2+}	Na^{+}	K^{+}	HCO_3^{-}	Cl^{-}	NO_3^{-}	SO_4^{2-}	Si	$\delta^{18}O$	$\delta^{2}H$	DIC	$\delta^{13}C_{DIC}$	DOC	$\delta^{13}C_{DOC}$	log pCO_2	^{3}H
			µS/cm	°C	m	mg/L										‰ VSMOW		mg/L C	‰ VPDB	mg/L C	‰ VPDB		TU
Groundwater: lower aquifer																							
Pz4	22/07/2013	7.7	–	2.8	4.89	143.77	22.00	5.30	1.90	9.10	70.67	10.00	0.4	21	3.8	−14.64	−103.7	–	–	–	–	−2.2	8.4
Pz4	09/07/2014	8.0	–	5.9	5.84	157.94	22.00	5.80	11.00	1.90	78.84	11.00	0.5	24	3.40	−14.95	−107.1	–	–	–	–	−3.2	–
Pz4	10/07/2015	7.3	216	6.8	4.60	141.08	22.00	5.70	11.00	1.10	71.98	12.00	0.4	25	3.30	−16.00	−114.7	9.5	−13.37	0.9	−25.29	−2.5	8.4
Pz4	29/06/2016	7.2	203	–	4.04	124.95	20.00	4.80	9.30	0.95	59.00	9.10	0.4	19	2.80	−15.89	−114.0	13.5	−12.0	1.2	−28.2	−2.5	–
Pz6	12/07/2013	7.2	–	9	15.63	106.85	13.00	3.80	6.00	2.30	64.55	5.90	0.2	7	4.3	−14.48	−102.6	–	–	–	–	−2.5	8.6
Pz6	09/07/2014	7.5	–	7.4	16.01	101.53	13.00	3.80	6.20	1.80	59.63	6.70	0.3	6	4.40	−15.24	−108.6	–	–	–	–	−2.9	–
Pz6	10/07/2015	7.4	125	11.1	15.29	87.45	13.00	3.60	6.50	0.87	53.68	6.20	0.2	6	4.10	−15.74	−112.5	10.2	−17.18	2.7	−30.2	−2.8	–
Pz6	30/06/2016	6.8	129	1.37	13.33	80.13	12.00	3.50	6.40	0.83	42.00	5.20	0.23	7	3.10	−15.30	−109.2	10.6	−14.8	1.3	−28.2	−2.3	–
Pz8	17/07/2013	8.8	–	2.8	21.65	105.30	17.00	3.80	5.80	2.20	64.50	3.90	0.3	5	3.1	−13.23	−95.3	–	–	–	–	–	8.8
Pz8	25/06/2014		–	4.3	21.58	116.41	17.00	3.90	5.70	8.20	62.61	4.70	0.4	12	2.30	−13.69	−97.6	–	–	–	–	–	–
Pz8	08/07/2015	7.4	132	4.8	21.27	91.92	14.00	3.50	7.00	1.10	62.22	3.90	0.6	4	3.20	−14.80	−106.4	12.4	−7.82	1.2	−25.95	−2.7	–
Pz8	01/07/2016	8.0	121	0.52	21.05	76.80	12.00	2.90	5.90	1.00	46.00	2.80	0.3	3	3.30	−14.92	−106.9	10.5	−10.8	1.4	−27.8	−3.5	–
Pz9	10/07/2014	7.5		10.5	33.23	90.90	12.00	4.00	5.20	0.99	58.41	6.40	0.2	<3	3.90	−15.10	−107.3	–	–	–	–	−2.8	–
Pz9	10/07/2015	7.5	115	7.2	33.11	80.56	12.00	3.90	4.30	0.66	54.90	5.60	0.2	<3	3.50	−15.59	−110.5	11.3	−14.21	1.1	−26.83	−2.9	8.8
Pz9	06/07/2016	6.6	108	2.07	32.70	66.05	10.00	3.20	4.00	0.55	38.00	4.60	0.1	2.3	3.40	−15.11	−106.8	10.0	−13.2	1.6	−28.5	−2.2	–
Groundwater: upper aquifer																							
Pz2	15/07/2013	6.5	21	9.4	3.74	32.30	3.80	1.10	3.50	0.77	14.63	5.30	0.1	<3	3.2	−15.76	−111.2	–	–	–	–	−2.42	8.6
Pz2	27/06/2014	6.7	12	21.4	4.57	53.62	6.00	1.40	4.10	0.73	25.59	4.10	<0.1	8	3.70	−14.52	−102.4	–	–	–	–	−2.39	–
Pz2	09/07/2015	5.8	40	<10	3.59	23.62	2.80	0.83	3.50	0.37	13.42	3.30	0.1	<3	2.90	−16.78	−116.2	4.7	−22.40	1.4	−28.33	–	8.6
Pz2	02/07/2016	6.1	51	0.41	3.72	24.79	3.60	1.00	3.50	0.39	7.00	5.90	0.1	1	2.30	−16.32	−116.4	4.6	−21.5	2.1	−28.4	−2.4	–
Pz1405	11/07/2015	6.7	52	1.1	1.74	26.42	3.60	1.10	4.30	0.42	12.20	6.30	0.10	<3	2.80	−18.94	−133.8	3.8	−22.52	2.1	−28.73	–	–
Pz1405	07/07/2016	5.9	36	2.8	2.06	17.92	2.00	0.57	2.70	0.25	6.00	3.10	0.08	0.9	2.40	−18.82	−135.9	2.8	−20.5	2.2	−28.3	−2.3	–
Pz1404b	12/07/2015	7.5	38	4.1	3.36	21.08	2.70	0.70	3.10	0.42	9.76	4.00	0.10	<3	3.50	−16.92	−120.1	1.9	−15.74	1.0	−28.03	−3.6	–
Pz1404b	07/07/2016	6.5	35	5.9	3.48	20.33	2.60	0.66	2.30	0.37	8.00	2.20	0.08	1	3.20	−17.66	−126.9	2.3	−17.4	1.2	−28.0	−2.7	–
Pz1402	12/07/2015	5.2	33	6.1	1.49	14.06	1.20	0.68	2.90	0.42	3.66	6.20	<0.1	<3	1.90	−19.26	−135.6	3.5	−25.9	1.5	−28.56	–	–
Pz1402	06/07/2016	5.5	21	4.8	1.64	11.06	0.61	0.32	1.80	0.23	3.00	2.10	<0.02	1.5	1.50	−17.15	−123.6	2.4	−24.7	2.3	−28.3	−2.1	–
PzDP	13/07/2015	6.1	38	2.3	3.43	20.61	2.90	0.71	2.80	0.32	10.98	3.70	<0.1	<3	2.00	−19.30	−135.9	3.1	−19.36	1.2	−28.19	–	–
PzDP	07/07/2016	6.2	40	6	3.94	19.34	2.60	0.60	2.30	0.24	6.00	4.70	0.15	1	1.90	−18.47	−132.4	–	–	–	–	−2.5	–
Stream water																							
Outlet	10/07/14	7.6	17	7.1	–	77.09	9.50	3.50	5.30	1.10	36.49	6.70	<0.1	11	3.50	−16.91	−121.5	–	–	–	–	–	–
Outlet	12/07/2015	8.7	94	4.8	–	57.34	8.20	2.90	4.70	1.00	26.84	5.40	<0.1	10	3.00	−17.35	−124.9	4.9	−11.73	2.9	−28.44	−4.4	–
Outlet	05/07/2016	7.6	134	3.6	–	74.90	11.00	3.90	5.40	1.40	30.00	5.40	0.06	14	3.80	−15.96	−115.3	–	–	–	–	−3.2	–
Outlet	09/07/2016	7.4	165	6.2	–	96.00	15.00	4.80	5.70	1.50	41.00	5.90	0.08	18	4.10	−15.96	−115.6	10.2	−11.1	3.0	−28.7	−2.9	–

Cl^- compared to the other wells. Further similarities and differences between the hydrogeochemistry of the lower aquifer and stream water can be noted from their Stiff diagrams (Fig. 3b). Based on the Piper and Stiff diagrams, four water types can be identified:

1. Very low TDS groundwater in the surficial aquifer with significant inter-annual variability
2. Water from wells Pz8, Pz9 and Pz6, with little inter-annual variability
3. Water from well Pz4, which is more mineralized than upgradient groundwater samples
4. Stream water

Trace elements (identified in section 'Sampling campaign') were also analysed to assess the water quality for potential use as drinking water. Within the scope of our analysis, no samples exceeded the Canadian drinking water standard (Health Canada 2017).

Water isotopes

To develop a framework for comparison of water isotope data within the watershed (Table 1), the LMWL was first established based on 2 years of monthly sampling of precipitation (rain and snow) at the Umiujaq airport. Eight samples were discarded due to signs of evaporation during and after sampling. The isotope dataset of precipitation ranges from a maximum $\delta^{18}O_{H2O}$ value of −10.4‰ and a maximum $\delta^{2}H_{H2O}$ value of −70.3‰ (rain, September 2015) to a minimum $\delta^{18}O_{H2O}$ value of −30.7‰ and a minimum $\delta^{2}H_{H2O}$ value of −235.8‰ (snow, December 2015). The linear regression for assessing the LMWL at Umiujaq, based on 15 samples with a coefficient of determination R^2 of 0.998, is expressed as:

$$\delta^{2}H_{H2O} = 8.03\ \delta^{18}O_{H2O} + 10.35 \quad (1)$$

which is close to the global meteoric water line, GMWL (Craig 1961; Rozanski et al. 1993).

Except for water from the lakes, all samples are located along the LMWL (Fig. 4). Snow is the most isotopically depleted component ranging from −30.7‰ $\delta^{18}O_{H2O}$ (−235.8‰ $\delta^{2}H_{H2O}$) to −18.8‰ $\delta^{18}O_{H2O}$ (−141.2‰ $\delta^{2}H_{H2O}$) with an average of −22.9‰ $\delta^{18}O_{H2O}$ (−149.8‰ $\delta^{2}H_{H2O}$). Isotopes of snow samples taken directly from the snow cover within the watershed in March 2015 and April 2016 are slightly above the LMWL. This enrichment in $\delta^{2}H_{H2O}$ is currently difficult to explain but may be due to post-depositional processes affecting the isotope ratio, mainly sublimation of snow and evaporation of meltwater (Christner et al. 2017). Nevertheless, these small shifts do not affect the overall conclusions drawn from the isotope data set.

Measured δ-values in water samples taken from lakes in the Tasiapik Valley watershed vary from −17.8‰ $\delta^{18}O_{H2O}$ (−129.7‰ $\delta^{2}H_{H2O}$) to −9.44‰ $\delta^{18}O_{H2O}$ (−81.5‰ $\delta^{2}H_{H2O}$) with an average of −12.8‰ $\delta^{18}O_{H2O}$ (−99.7‰ $\delta^{2}H_{H2O}$) (Fig. 4b). A local evaporative line (LEL) was defined from a linear regression through the previous measured δ-values The crossover point between this LEL and the LMWL has a value of −15.4‰ for $\delta^{18}O_{H2O}$ (−113.3‰ $\delta^{2}H_{H2O}$) and represents the isotopically-weighted average of annual precipitation (Wolfe et al. 2007).

Rain isotope ratios vary between −17.3‰ $\delta^{18}O_{H2O}$ (−134.2‰ $\delta^{2}H_{H2O}$) and −8.7‰ $\delta^{18}O_{H2O}$ (−65.2‰ $\delta^{2}H_{H2O}$) with an average of −12.6‰ $\delta^{18}O_{H2O}$ (−92.0‰ $\delta^{2}H_{H2O}$). Stream water has an isotope ratio varying from −17.4‰ $\delta^{18}O_{H2O}$ (−125.6‰ $\delta^{2}H_{H2O}$) to −15.4‰ $\delta^{18}O_{H2O}$ (−111.0‰ $\delta^{2}H$) with an average of −16.4‰ $\delta^{18}O_{H2O}$ (−118.2‰ $\delta^{2}H_{H2O}$; Fig. 4b–c).

Groundwater samples fall in the range of local rain variations, ranging from −19.3‰ $\delta^{18}O_{H2O}$ (−135.9‰ $\delta^{2}H_{H2O}$) to −14.5‰ $\delta^{18}O_{H2O}$ (−102.4‰ $\delta^{2}H_{H2O}$) with an average of −17.5‰ $\delta^{18}O_{H2O}$ (−124.0‰ $\delta^{2}H_{H2O}$) in the upper surficial aquifer, and from −16.00‰ $\delta^{18}O_{H2O}$ (−114.7‰ $\delta^{2}H_{H2O}$) to −13.23‰ $\delta^{18}O_{H2O}$ (−95.3‰ $\delta^{2}H_{H2O}$) with an average of −15‰ $\delta^{18}O_{H2O}$ (−106.9‰ $\delta^{2}H_{H2O}$) in the lower aquifer (Fig. 4c–d).

Ground ice in two of the permafrost mounds at a depth of 5 m below the active layer has isotope values between −15.4‰ $\delta^{18}O_{H2O}$ (−111.2‰ $\delta^{2}H_{H2O}$) and −12.9‰ $\delta^{18}O_{H2O}$ (−91.1‰ $\delta^{2}H_{H2O}$) with an average of −14.4‰ $\delta^{18}O_{H2O}$ (−103.0‰ $\delta^{2}H_{H2O}$; Fig. 4c). These δ-values are similar to other isotope measurements in ground ice from the wider Umiujaq area (Calmels et al. 2008; Narancic et al. 2017).

DIC, DOC, $\delta^{13}C_{DIC,DOC}$ and pCO_2

Characterising the carbon species in a watershed is useful for interpreting recharge and weathering processes. DIC and DOC concentrations in the watershed as well as their $\delta^{13}C$ isotope values in the stream, and in the deep and shallow groundwater, are presented in Fig. 5a.

DOC concentrations in groundwater vary from 0.9 to 3.4 mg/L C. Measured DOC is higher in the stream, ranging from 1.78 to 5.45 mg/L C, and decreases from the upstream part of the stream to the outlet. The $\delta^{13}C_{DOC}$ isotope ratio, however, remains stable in both the stream and groundwater, with an average ratio of −28.1‰ VPDB, which can be attributed to the $\delta^{13}C_{DOC}$ value of soil in a C3-type vegetation environment.

DIC concentrations are more variable within and between the different water compartments. Groundwater in the surficial aquifer has the lowest DIC concentrations, ranging from 1.9 to 4.7 mg/L C, while DIC concentrations vary from 9.6 to 13.5 mg/L C in the lower aquifer (Fig. 5a). In the stream, DIC concentrations vary between 4.9 and 10.2 mg/L C.

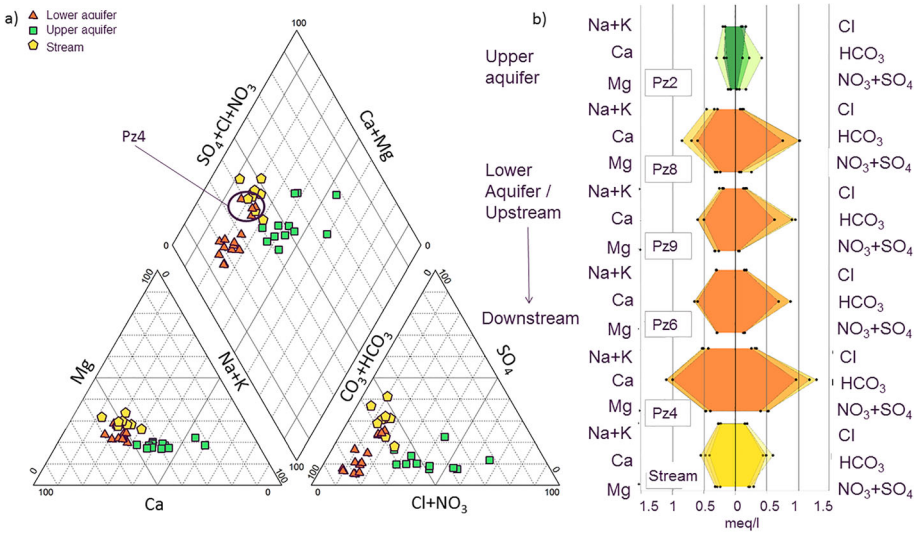

Fig. 3 Hydrogeochemical data of the Tasiapik Valley watershed at Umiujaq: **a** Piper diagram of groundwater from the upper surficial and lower aquifers as well as from stream water of the watershed, and **b** Stiff diagrams for water samples taken in 2014, 2015, and 2016 from lightest to darkest color, respectively. For simplicity, the Stiff diagram only includes data from the five monitor wells and the stream, whereas the Piper plot also includes the piezometers. All data are provided in Table 1

The shallow groundwater $\delta^{13}C_{DIC}$ ratios range from −15.7 to −25.9‰ VPDB, while deep groundwater has $\delta^{13}C_{DIC}$ ratios between −7.8 and −17.2‰ VPDB. The stream water $\delta^{13}C_{DIC}$ values are within the range of deep groundwater (from −11.1 to −14.2‰ VPDB). Mean pCO_2 values for shallow and deeper groundwater are $10^{-2.6}$ atm (Table 1), which is in the range of dry and low organic soils (Clark 2015) and consistent with the values presented by Kessler and Harvey (2001) for soils of northern regions. The mean stream water pCO_2 is $10^{-3.4}$ atm, which appears to be in equilibrium with atmospheric values (Clark 2015). pH values in groundwater range from 6.6 to 8.8 in the lower aquifer and from 5.2 to 7.5 in the surficial aquifer. Figure 5b shows the $\delta^{13}C_{DIC}$ and pH values of groundwater samples and the PHREEQC-calculated pCO_2 equilibration lines for an open system.

Dating

The $^3H/^3He$ age dating method was used to estimate groundwater residence times in the aquifers. Unfortunately, reliable tritiogenic ^3He concentrations could not be obtained because of significant excess air in the samples, which suggests rapid recharge. Nevertheless, since groundwater in the watershed has ^3H (tritium) concentrations ranging from 8.4 ± 0.3 to 8.8 ± 0.3 TU, it was concluded that groundwater is indeed recharged by modern water (Clark and Fritz 1997).

Discussion

Hydrogeochemical conceptual model

A conceptual flowchart of the hydrogeochemical system of the Tasiapik Valley watershed at Umiujaq, including components of groundwater recharge and infiltration, geochemical evolution and groundwater discharge, was developed based on detailed field observations including a chemical analysis of precipitation, groundwater, surface water and permafrost (Fig. 6). This conceptual model is described in the following.

Surficial groundwater

In the upper part of the watershed, groundwater in the surficial aquifer has very low TDS concentrations and shows significant variations, both in terms of hydrogeochemical water types and between different piezometers (Table 1; Fig. 3). The low TDS concentrations can be explained by the short travel times within this aquifer, while the proximity of the watershed to Hudson Bay could explain the water-type variations. Hudson Bay is a saltwater inland sea that provides a source of Na^+ and Cl^-, in aerosol form, for local precipitation in the watershed.

Groundwater becomes enriched in CO_2 during recharge through soils (Utting et al. 2013). For the surficial groundwater, pCO_2 values are around $10^{-2.6}$ atm, which is higher than atmospheric pressure and surface water pCO_2 ($10^{-3.4}$ atm). According to Clark (2015), these pCO_2 values are typical for dry and low-organic soils. Measured $\delta^{13}C_{DOC}$ values (Fig. 5) also confirm the soil influence as its signature is related to C3 vegetation (Clark and Fritz 1997).

DIC concentrations in the upper surficial aquifer are lower than in the lower aquifer, while $\delta^{13}C_{DIC}$ values (Fig. 5) reflect that the soil CO_2 is dominated by C3-type vegetation (Vogel 1993). Moreover, water stable isotope values in the surficial aquifer are more influenced by snowmelt water than in the lower aquifer (Fig. 4).

The tritium concentration of 8.6 TU measured in the surficial aquifer can be considered as an indication of modern recharge (Clark and Fritz 1997), which is also consistent with the seasonal water level variations

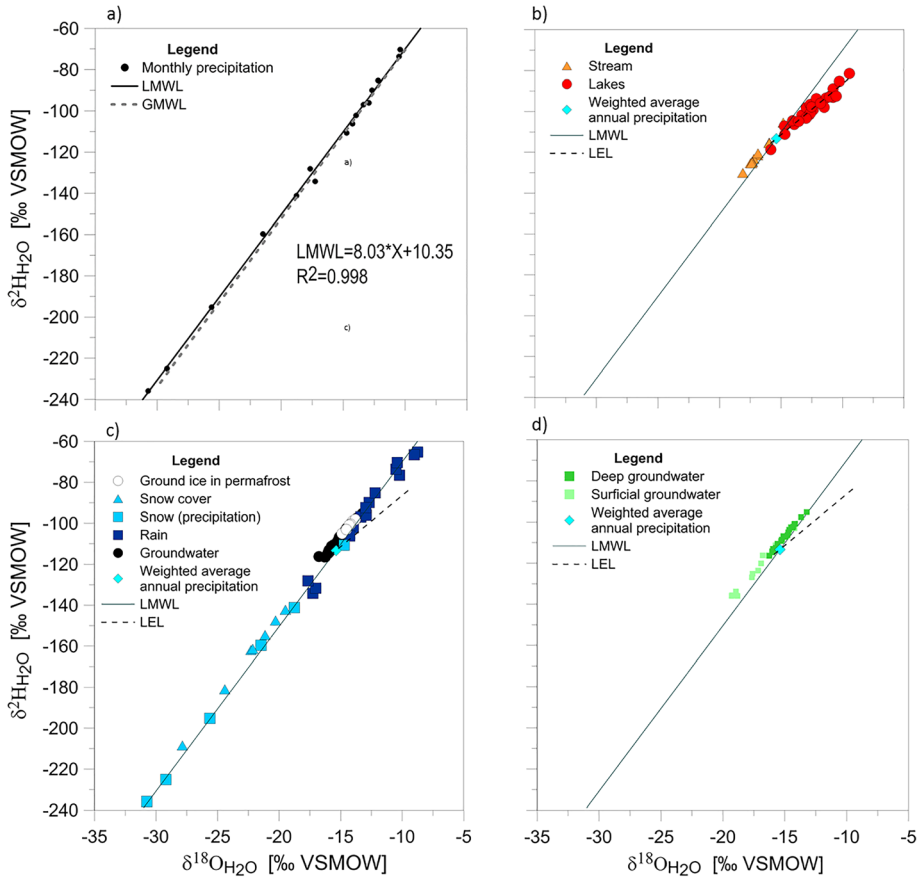

Fig. 4 Stable isotopes measured in water samples from different sources in the Tasiapik Valley watershed at Umiujaq: **a** monthly precipitation data, **b** stream data, **c** combined precipitation, groundwater from the lower aquifer, and ground ice in permafrost, and **d** groundwater from the upper and lower aquifers. Each figure includes the local meteoric water line (LMWL) for Umiujaq assessed from monthly precipitation sampling at the Umiujaq airport from July 2014 to July 2016. The black-dashed line represents the local evaporative line (LEL) assessed from isotopes measured in water samples taken from lakes within the watershed. The grey-dashed line represents the global meteoric water line (GMWL), according to Craig (1961) and Rozanski et al. (1993)

observed in the surficial aquifer piezometers (Lemieux et al. 2020, this issue). Higher groundwater levels during the snowmelt period (May–July) indicate recharge while lower groundwater levels during the frozen period (October–May) are associated with depletion of stored groundwater in the absence of recharge. Well hydrographs in the surficial aquifer show that it dries up almost completely in winter. The observed data, including seasonal variations in the well hydrographs, low TDS concentrations, variations in the hydrogeochemical facies, as well as the water stable isotope data, suggest a complete renewal of surficial groundwater every year. Recharge seems to originate mainly from snowmelt water which rapidly infiltrates into low organic content soil. Variations in hydrogeochemical water types between piezometers suggest a heterogeneous aquifer with possible small discontinuous aquifer units of littoral sand (Mb) located within depressions of the marine silt (Ma; Fig.

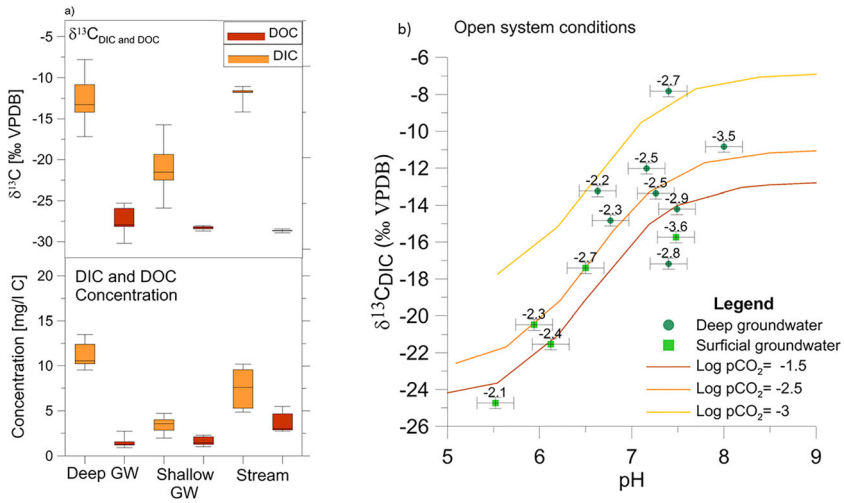

Fig. 5 Carbon chemistry of water samples at Umiujaq: **a** Carbon phases, DOC, DIC and their $\delta^{13}C$ values, and **b** observed $\delta^{13}C_{DIC}$ as a function of pH with theoretical pCO_2 evolution in an open system. Calculated pCO_2 values are presented above each data point

2). There is no evidence of a direct connection between the upper and lower aquifers, which is expected since the upper aquifer is underlain by the marine silt unit (Ma) and by a thick unsaturated zone that likely acts as a capillary barrier between these aquifers.

Deep groundwater

The lower aquifer is generally unconfined in the upper part of the watershed and confined in the lower part, with seasonal artesian conditions at well Pz4 (Fig. 2). Lemieux et al. (2020, this issue) show that the hydrographs for wells Pz6 and Pz4 in the confined lower aquifer in the lower part of the watershed show significant seasonal variations between the maximum (December–January) and minimum (May–June) water levels. These variations result from the aquifer confinement and proximity of these wells to the watershed discharge zone, which leads to a funnel effect for incoming groundwater flowing from the upper part of the valley and transversely from the cuesta. The dominant hydrogeochemical water type for all wells in the lower aquifer is Ca-HCO_3 and the TDS content ranges from 66 to 158 mg/L.

Measured pCO_2 and $\delta^{13}C_{DOC}$ values also confirm recharge through soils with low organic matter contents that are composed of C3 organic matter. Increases in DIC concentrations, and $\delta^{13}C_{DIC}$ values more positive than −17‰ (Fig. 5a), can be interpreted as the deeper groundwater representing closed-system weathering of carbonates (Utting et al. 2013). This interpretation is confirmed by the data shown in Fig. 5b where only well Pz4 appears to be in an open system, at $pCO_2 = 10^{-2.5}$ atm, and where calculated pCO_2 and equilibration lines appear to be in good agreement. All other samples in the lower aquifer do not seem to correspond to open-system equilibration lines (Fig. 5b) and therefore likely belong to a closed system. Similar approaches have been taken in other catchment studies (Cronin et al. 2005). Although carbonates are locally present in veins and fractures of the underlying bedrock and in sedimentary rock formations within the Nastapoka Group (ex. along the cuesta ridge; Fortier et al. 2020, this issue), no value for a carbon isotope end-member in carbonate could be determined. Therefore, a closed-system scenario remains likely for the lower aquifer, but clear isotope values could not be associated with the calculated model. The apparent open system for well Pz4 is surprising since it lies at the end of a groundwater flow path and should carry a closed-system history as in the other groundwater samples; its signature may indicate an admixture of groundwater fluxes from other sources.

Water stable isotopes of deeper groundwater scatter close to the weighted average of annual precipitation (Fig. 4). Tritium concentrations vary between 8.4 ± 0.3 and 8.8 ± 0.3 TU, which is an indication of modern recharge (Clark and Fritz 1997). Measured seasonal variations in piezometric levels also suggest modern recharge with a 6-month delay between the peak recharge season during snowmelt and the higher piezometric levels measured in wells Pz6 and Pz4 in winter (Lemieux at al. 2020, this issue). Based on these observations, groundwater in the lower aquifer appears to be recharged by modern precipitation. Groundwater sampled in the area can be considered as young with a poorly evolved hydrogeochemical composition and low mineralisation. No evidence of meltwater infiltration into the lower aquifer from degradation of permafrost ground ice was found within the framework of this study. This finding is consistent with the conceptual model presented by Lemieux et al. (2020, this issue), which indicates that in the upper part of the valley where the permafrost-rich silt unit is present, downward groundwater flow toward the lower aquifer is restricted by the capillary barrier effect of the thick unsaturated zone. In the lower part of the valley, where the lower aquifer is confined, groundwater flows upward across the permafrost-rich silt unit, from the lower aquifer toward the stream. Meltwater from ground ice is therefore not flowing toward the lower aquifer, but rather toward the stream.

Observed differences in groundwater hydrogeochemistry and increases in TDS between wells Pz6 and Pz4 are interpreted, together with open-system weathering conditions and a more irregular well hydrograph at well Pz4 (Lemieux et al. 2020, this issue), as indications of mixing between the deep groundwater and another groundwater source in the lower part of the watershed. One hypothesis for this contribution is water infiltration through the highly fractured surface of the cuesta with a significant recharge peak during snowmelt that also enables rapid CO_2 exchange. This is also compatible with the conceptual model of Lemieux et al. (2020, this issue) which suggests that groundwater from the cuesta ridge flows toward the lower aquifer. In their 2D numerical model, Dagenais et al. (2020, this issue) also assume that flow occurs primarily within the transverse direction toward the central stream and includes the cuesta ridge as an important recharge zone for the lower aquifer. This hypothesis could be confirmed in the future with a tracer test at the edge of the cuesta.

Stream water

Since the hydrogeochemical composition of the stream and groundwater at well Pz4 is similar, with slight differences that seem primarily linked to dilution, the electrical conductivity was measured along the stream to verify if groundwater from the lower aquifer contributes significantly to the stream discharge. The measured EC along the 630-m-long profile increases from 39 to 165 µS/cm, from upstream to the downstream watershed outlet (Fig. 7). The measured EC profile is influenced by a small spring that discharges into the stream, at approximately 1 L/min. The spring has a Ca-HCO_3 water

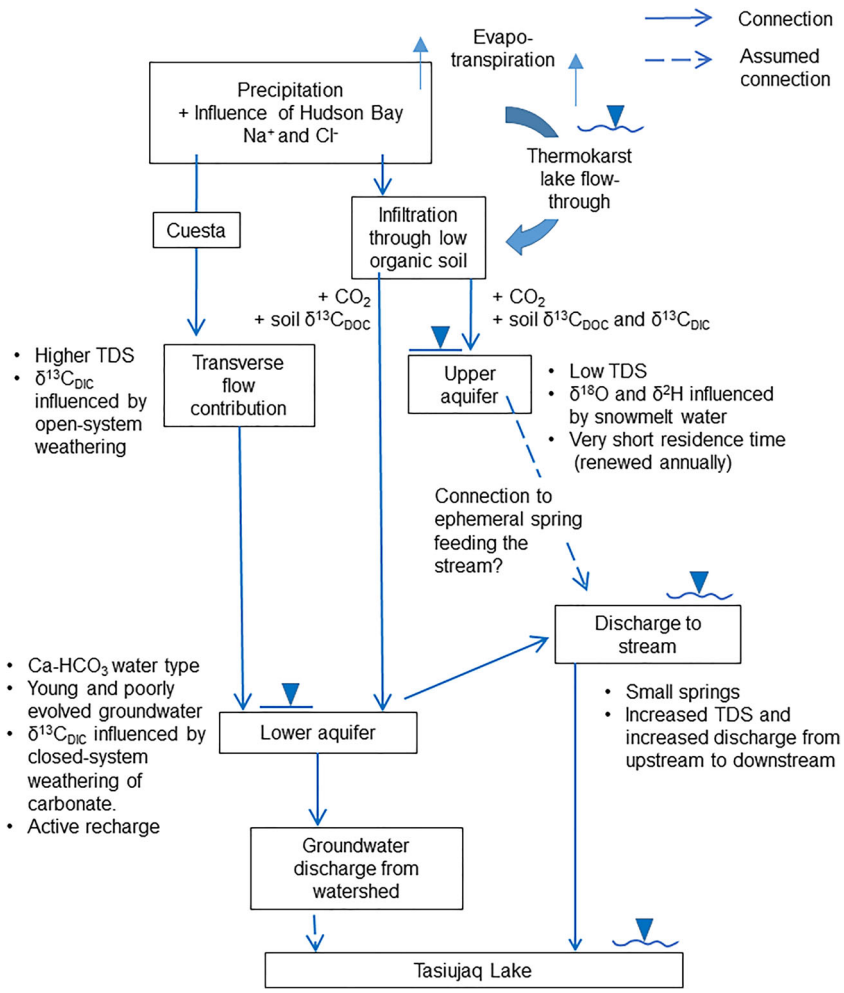

Fig. 6 Conceptual flowchart of the hydrogeochemical system within the Tasiapik Valley watershed at Umiujaq

type, 266 mg/L TDS and an EC of 425 µS/cm. The stream EC increased from 70 µS/cm at a distance of 50 m upstream of the intersection with the spring (shown in Fig. 7) to 110 µS/cm about 50 m downstream of the intersection.

The salt dilution tests showed that discharge increases by a factor of 5 along the stream, from 2 L/s upstream to 10.1 L/s at the watershed outlet (Fig. 7). A small tributary that originates at the foot of the permafrost mounds contributes about 2.5 L/s to the total discharge. This gradual increase in stream discharge provides further evidence that it is mainly fed by groundwater from the lower confined aquifer. This is also compatible with the findings of Lemieux et al. (2020, this issue) who showed that a significant contribution of groundwater baseflow from the lower aquifer contributes to the stream discharge.

Ground ice isotope signatures in permafrost mounds

Isotope ratios of ground ice in two permafrost mounds were analysed to provide insight into permafrost aggradation and to find a possible tracer for meltwater of ground ice. Ground ice at depths ranging from 1.5 to 5 m within the permafrost mounds has $\delta^{18}O_{H2O}$ and $\delta^{2}H_{H2O}$ ratios within the range of modern water (rain and groundwater) on the LMWL (Fig. 4). Calmels et al. (2008) and Narancic et al. (2017) observed similar values for ground ice at another study site located 16 km east of the watershed, in the Sheldrake River Valley. Their site is also located in discontinuous permafrost where seasonal or historically recent freeze–thaw events affecting the shallow permafrost below the active layer can induce water mixing between recently recharged groundwater and permafrost water. Having aggraded under colder-climate conditions, shallow permafrost with originally depleted $\delta^{18}O_{H2O}$ and $\delta^{2}H_{H2O}$ values can therefore become isotopically enriched by such groundwater addition (Banville 2016; Calmels et al. 2008; Fallu et al. 2005; Kerwin et al. 2004).

Modern water infiltration into near-surface permafrost could have been more clearly identified using ^{3}H signatures but such analyses were not carried out in the present study. However, measured ^{3}H values down to a depth of 5 m in a lithalsa (a permafrost mound without peat cover) near the Umiujaq watershed range from 2.5 ± 0.6 TU to 1.9 ± 0.5 TU, which clearly indicates modern water infiltration into the superficial permafrost layer (Calmels et al. 2008). Modern water

infiltration into permafrost was attributed to seasonal water movement affecting near-surface permafrost (Kokelj and Burn 2003), including temperature-induced downward moisture migration (Burn and Michel 1988; Cheng 1983). Moreover, the recent marked trend to climate warming is also inducing an increase in the unfrozen water content in permafrost (Calmels et al. 2008).

Implications for drinking water

The evolution of groundwater quality in degrading permafrost environments is a growing concern, as the expected development of northern regions will likely increase the need for new drinking water supplies (Cochand et al. 2019). Within the framework of this study, hydrogeochemical evolution and weathering processes were found to be similar to those in nonpermafrost environments. Results were also consistent with other studies on groundwater quality in permafrost areas (Utting et al. 2013; Williams 1970). The groundwater system in the watershed at Umiujaq shows dynamic recharge and high renewal rates. Significant groundwater flow rates in the upper and lower aquifer have been measured, for example, by Jamin et al. (2020, this issue) using the finite volume point dilution method. Moreover, groundwater meets the Canadian quality standards for drinking water (Health Canada 2017). However, even if permafrost is currently degrading in this watershed, recharge into the lower aquifer will probably not increase significantly due to the presence of the confining marine silt unit (Ma). This particular site might therefore not be suitable as a water supply. Another issue also concerns the cost of transporting water from the watershed, which is about 8 km from the Inuit community of Umiujaq (Fig. 1).

Nevertheless, these preliminary results are promising for locating water sources in similar hydrogeological contexts in other communities, in that their groundwater resources will likely be of similar excellent quality and potentially good sources of drinking water. However, in this context, particular attention should be paid to the vulnerability of shallow groundwater systems as rapid recharge dynamics associated with thin soil layers and the loss of the permafrost confining layer may increase the risk of groundwater to potential contamination.

Conclusions and perspectives

The use of various environmental tracers, including major ions, DIC, DOC, water and carbon stable isotopes and ^{3}H, has allowed a detailed characterisation of groundwater flow behavior and quality in a watershed within a discontinuous permafrost zone in Nunavik (Québec), Canada. Shallow groundwater located in small isolated depressions filled with sand, forming an unconfined aquifer, is young and poorly evolved. This unconfined aquifer appears to be renewed every year and is mainly recharged by snowmelt infiltration through low-organic soil. Deeper groundwater that is partially confined by a marine silt unit which has been partially invaded by permafrost, is also recharged by modern precipitation and is also considered young.

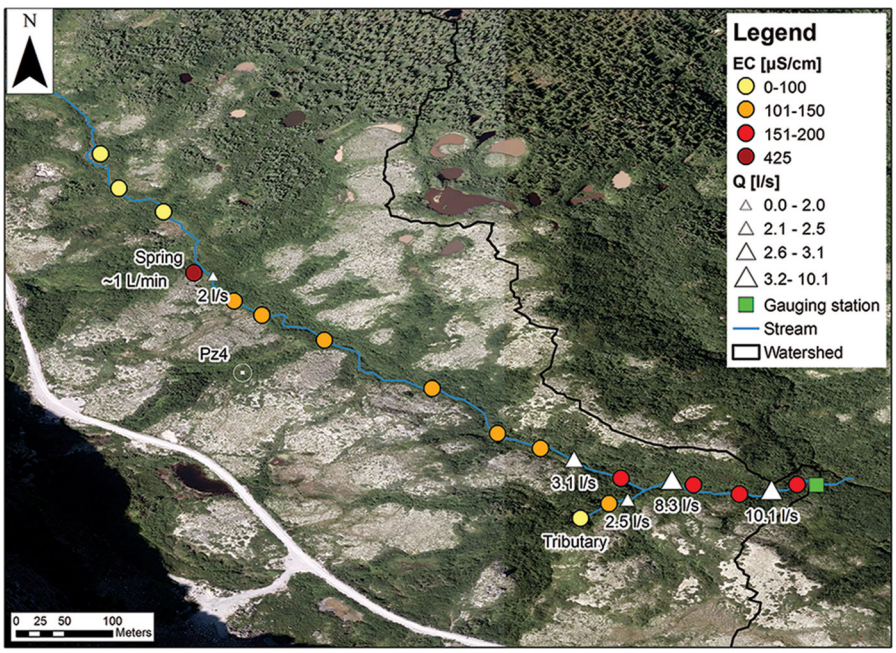

Fig. 7 EC-profile and discharge measurements along the stream in the Tasiapik Valley watershed at Umiujaq. The gauging station is located at the watershed outlet

Carbon isotope data show evidence of carbonate dissolution in a closed system. Only the downstream piezometer Pz4 shows open-system conditions, which are associated with changes in hydrogeochemistry and piezometry. These changes are interpreted as contributions from other groundwater sources in the aquifer, possibly including infiltration through the highly fractured cuesta ridge.

Within the framework of this study, due to the absence of a unique isotope signature within the shallow permafrost zone, and in part because of the short time scale of the study, it was not possible to identify the contributions of meltwater to the lower aquifer from degradation of permafrost ground ice.

Close to the watershed outlet, hydrogeochemical data and discharge measurements show evidence of a significant contribution of deep groundwater to the stream, originating from the confined aquifer below the permafrost mounds. These results are consistent with the conceptual model of Lemieux et al. (2020, this issue) and the coupled groundwater flow–heat transfer model of Dagenais et al. (2020, this issue), which showed significant groundwater flow in the confined aquifer below one of the downgradient permafrost mounds, and discharge to the stream.

The LMWL for Umiujaq was determined based on 2 years of monthly precipitation sampling and is close to the Global Meteoric Water Line (GMWL). Although ground ice sampled in the first 5 m in ice-rich permafrost mounds has water $\delta^{18}O_{H2O}$ and $\delta^{2}H_{H2O}$ ratios within the range of modern precipitation, further investigations based on ice ^{3}H content are needed to confirm modern infiltration of water into these permafrost mounds.

Although groundwater in the lower aquifer meets the Canadian quality standards for drinking water, groundwater from this particular site might not be suitable as a water supply due to the confining silt layer which limits recharge, due to limited available volumes, and the significant distance to the Inuit community of Umiujaq. Nonetheless, in the current context of permafrost degradation due to climate warming as observed throughout Nunavik (Québec) and elsewhere in the circumpolar world, the use of groundwater in degrading permafrost areas should be considered for supplying drinking water to users such as northern communities and mining companies. In this perspective, particular attention to the release of toxic elements such as mercury, which has been associated with permafrost degradation (Schuster et al. 2018), should also be considered in further studies. In addition, vulnerability of this resource should be carefully evaluated, and suitable protection areas, accounting for possible recharge through discontinuous permafrost, will need to be delimited for associated water supply wells, as they are in southern regions.

Processes associated with hydrogeochemical evolution of groundwater and weathering within the Tasiapik Valley watershed are similar to those in nonpermafrost environments. At this particular site, the discontinuous permafrost does not have a strong confining effect. Further studies should include annual surveys of groundwater quality evolution. The hydrogeochemical data set from this study will be very useful as a baseline for comparison with future studies at Umiujaq and in similar regions to document climate-change-induced impacts of permafrost degradation on hydrogeological systems.

Acknowledgements We would like to thank everyone who helped us in this study during the field work and data collection, especially Renaud Murray, Marie-Catherine Talbot Poulin, Pierre Jamin, Sophie Dagenais, Pierrick Lamontagne-Hallé, Shuai Guo, Masoumeh Parhizkar, and Jonathan Sottas. Pierre Therrien provided valuable technical support for data treatment. Finally, we would like to thank the Inuit community of Umiujaq, in particular Ernest Tumic and Darleen MacDougal, for their help and collaboration on this project.

Funding information We acknowledge funding from a Strategic Project Grant of the Natural Sciences and Engineering Research Council of Canada (NSERC), the Quebec Ministry of Environment (Ministère du développement durable, de l'environnement et de la lutte contre les changements climatiques – MDDELCC) and the Québec Research Fund (Fonds de recherche Nature et Technologies du Québec – FRQNT). We also acknowledge a travel grant from the Quebec Ministry of International Relations (Ministère des relations internationales et de la Francophonie – MRIF). Administrative and logistical support from the Centre d'études nordiques (CEN), Université Laval, is greatly appreciated.

References

Alexeev SV, Alexeeva LP (2003) Hydrogeochemistry of the permafrost zone in the central part of the Yakutian diamond-bearing province, Russia. Hydrogeol J 11:574–581. https://doi.org/10.1007/s10040-003-0270-8

Back W (1966) Hydrochemical facies and ground-water flow patterns in northern part of Atlantic Coastal Plain. US Geol Surv Prof Pap 498-A https://doi.org/10.3133/pp498A

Banville D-R (2016) Modélisation cryohydrogéologique tridimensionnelle d'un bassin versant pergélisolé, une étude cryohydrogéophysique de proche surface en zone de pergélisol discontinu à Umiujaq au Québec Nordique [Three-dimensional cryohydrogeological modeling of a permafrost watershed: a near-surface cryohydrogeophysical study in a discontinuous permafrost zone in Umiujaq, northern Quebec]. MSc Thesis, Université Laval, Québec City, Canada

Beck I, Ludwig R, Bernier M, Levesque E, Boike J (2015) Assessing permafrost degradation and land cover changes (1986–2009) using remote sensing data over Umiujaq, Sub-Arctic Quebec. Permafr Periglac Process 26:129–141. https://doi.org/10.1002/ppp.1839

Bense VF, Ferguson G, Kooi H (2009) Evolution of shallow groundwater flow systems in areas of degrading permafrost. Geophys Res Lett 36. https://doi.org/10.1029/2009GL039225

Blanchette D, Cloutier V, Roy M, Audet-Gagnon F, Castelli S, Beaudry C (2010) Protocole d'échantillonnage des eaux souterraines-Programme d'acquisition de connaissances sur les eaux souterraines au Québec (PACES) [Groundwater sampling protocol: Groundwater Knowledge Acquisition Program in Quebec]. UQAT, Rouyn-Noranda, Quebec, Canada

Bosson E, Selroos J-O, Stigsson M, Gustafsson L-G, Destouni G (2013) Exchange and pathways of deep and shallow groundwater in different climate and permafrost conditions using the Forsmark site,

Sweden, as an example catchment. Hydrogeol J 21:225–237. https://doi.org/10.1007/s10040-012-0906-7
Boucher JL, Carey SK (2010) Exploring runoff processes using chemical, isotopic and hydrometric data in a discontinuous permafrost catchment. Hydrol Res 41:508–519. https://doi.org/10.2166/nh.2010.146
Brown R, Lemay M, Allard M, Barrand EN, Barrette C, Bégin Y, Bell T, Bernier M, Bleau S, Chaumont D, Dibike Y, Frigon A, Leblanc P, Paquin D, Sharp M, Way R (2012) Climate variability and change in the Canadian Eastern Subarctic IRIS region (Nunavik and Nunatsiavut). In: Nunavik and Nunatsiavut: From science to policy. An Integrated Regional Impact Study (IRIS) of climate change and modernization. ArcticNet, Québec, QC
Burn CR, Michel FA (1988) Evidence for recent temperature-induced water migration into permafrost from the tritium content of ground ice near Mayo, Yukon Territory, Canada. Can J Earth Sci 25:909–915. https://doi.org/10.1139/e88-087
Callegary J, Kikuchi C, Koch J, Lilly M, Leake S (2013) Review: Groundwater in Alaska (USA). Hydrogeol J 21:25–39. https://doi.org/10.1007/s10040-012-0940-5
Calmels F, Gagnon O, Allard M (2005) A portable earth-drill system for permafrost studies. Permafr Periglac Process 16:311–315. https://doi.org/10.1002/ppp.529
Calmels F, Delisle G, Allard M (2008) Internal structure and the thermal and hydrological regime of a typical lithalsa: significance for permafrost growth and decay. Can J Earth Sci 45:31–43. https://doi.org/10.1139/e07-068
Carey S, Boucher J, Duarte C (2013) Inferring groundwater contributions and pathways to streamflow during snowmelt over multiple years in a discontinuous permafrost subarctic environment (Yukon, Canada). Hydrogeol J 21:67–77. https://doi.org/10.1007/s10040-012-0920-9
Cheng G, Jin H (2013) Permafrost and groundwater on the Qinghai-Tibet plateau and in Northeast China. Hydrogeol J 21:5–23. https://doi.org/10.1007/s10040-012-0927-2
Cheng GD (1983) The mechanism of repeated-segregation for the formation of thick layered ground ice. Cold Reg Sci Technol 8:57–66. https://doi.org/10.1016/0165-232X(83)90017-4
Chouinard C, Fortier R, Mareschal JC (2007) Recent climate variations in the subarctic inferred from three borehole temperature profiles in northern Quebec, Canada. Earth Planet Sci Lett 263:355–369. https://doi.org/10.1016/j.epsl.2007.09.017
Christner E, Kohler M, Schneider M (2017) The influence of snow sublimation and meltwater evaporation on delta D of water vapor in the atmospheric boundary layer of Central Europe. Atmos Chem Phys 17:1207–1225. https://doi.org/10.5194/acp-17-1207-2017
Claesson Liljedahl L, Kontula A, Harper J, Näslund J-O, Selroos J-O, Pitkänen P, Puigdomenech I, Hobbs M, Follin S, Hirschorn S, Jansson P, Kennell L, Marcos N, Ruskeeniemi T, Tullborg E-L, Vidstrand P (2016) The Greenland Analogue Project: final report. SKB - Swedish Nuclear Fuel and Waste Management Co, Stockholm
Clark ID (2015) Groundwater geochemistry and isotopes. CRC, Boca Raton, FL
Clark ID, Fritz P (1997) Environmental isotopes in hydrogeology. CRC, Boca Raton, FL
Clark ID, Lauriol B (1997) Aufeis of the Firth River basin, northern Yukon, Canada: insights into permafrost hydrogeology and karst. Arct Alp Res 29:240–252. https://doi.org/10.2307/1552053
Clark ID, Lauriol B, Harwood L, Marschner M (2001) Groundwater contributions to discharge in a permafrost setting, Big Fish River, N.W.T., Canada. Arct Antarct Alp Res 33:62–69. https://doi.org/10.2307/1552278
Cochand M, Molson J, Lemieux J-M (2019) Groundwater hydrogeochemistry in permafrost regions. Permafr Periglac Process. https://doi.org/10.1002/ppp.1998
Craig H (1961) Isotopic variations in meteoric waters. Science 133:1702–1703. https://doi.org/10.1126/science.133.3465.1702
Cronin AA, Barth JAC, Elliot T, Kalin RM (2005) Recharge velocity and geochemical evolution for the Permo-Triassic Sherwood Sandstone, Northern Ireland. J Hydrol 315:308–324. https://doi.org/10.1016/j.jhydrol.2005.04.016
Dagenais S, Molson J, Lemieux J-M, Fortier R, Therrien R (2020) Coupled cryo-hydrogeological modelling of permafrost dynamics near Umiujaq (Nunavik, Canada). Hydrogeol J https://doi.org/10.1007/s10040-020-02111-3
Douglas TA, Blum JD, Guo L, Keller K, Gleason JD (2013) Hydrogeochemistry of seasonal flow regimes in the Chena River, a subarctic watershed draining discontinuous permafrost in interior Alaska (USA). Chem Geol 335:48–62. https://doi.org/10.1016/j.chemgeo.2012.10.045
Evans SG, Ge S (2017) Contrasting hydrogeologic responses to warming in permafrost and seasonally frozen ground hillslopes. Geophys Res Lett 44:1803–1813. https://doi.org/10.1002/2016GL072009
Fallu MA, Pienitz R, Walker IR, Lavoiec M (2005) Paleolimnology of a shrub-tundra lake and response of aquatic and terrestrial indicators to climatic change in arctic Quebec, Canada. Palaeogeogr Palaeoclimatol Palaeoecol 215:183–203. https://doi.org/10.1016/j.palaeo.2004.07.006
Ford JD (2009) Dangerous climate change and the importance of adaptation for the Arctic's Inuit population. Environ Res Lett 4:024006. https://doi.org/10.1088/1748-9326/4/2/024006
Fortier R, Aubé-Maurice B (2008) Fast permafrost degradation near Umiujaq in Nunavik (Canada) since 1957 assessed from time-lapse aerial and satellite photographs. In: Proceedings 9th International Conference on Permafrost, vol 1, Fairbanks, AK, July 2008, pp 457–462
Fortier R, Lemieux J-M, Therrien R, Molson J, Cochand M (2017) Rapport de synthèse sur le déploiement du réseau Immatsiak à Umiujaq au Québec nordique pour le suivi des eaux souterraines en régions froides [Synthesis report on the deployment of the Immatsiak network in Umiujaq, northern Quebec for groundwater monitoring in cold regions]. Université Laval, Quebec City, QC
Fortier R, Banville DR, Lévesque R, Lemieux J-M, Molson J, Therrien R, Ouellet M (2020) Development of a three-dimensional geological model, based on Quaternary chronology, geological mapping, and geophysical investigation, of a watershed in the discontinuous permafrost zone near Umiujaq (Nunavik, Canada). Hydrogeol J https://doi.org/10.1007/s10040-020-02113-1
Frampton A, Painter SL, Destouni G (2013) Permafrost degradation and subsurface-flow changes caused by surface warming trends. Hydrogeol J 21:271–280. https://doi.org/10.1007/s10040-012-0938-z
Grosse G, Romanovsky V, Jorgenson T, Anthony KW, Brown J, Overduin PP (2011) Vulnerability and feedbacks of permafrost to climate change. Eos 92:73–74. https://doi.org/10.1029/2011EO090001
Health Canada (2017) Guidelines for Canadian drinking water quality: summary table. Health Canada, Ottawa, ON
Hounslow A (1995) Water quality data: analysis and interpretation. CRC, Boca Raton, FL
Jamin P, Cochand M, Dagenais S, Lemieux J-M, Fortier R, Molson J, Brouyère S (2020) Direct measurement of groundwater flux in aquifers within the discontinuous permafrost zone: an application of the finite volume point dilution method near Umiujaq (Nunavik, Canada). Hydrogeol J https://doi.org/10.1007/s10040-020-02108-y
Kerwin MW, Overpeck JT, Webb RS, Anderson KH (2004) Pollen-based summer temperature reconstructions for the eastern Canadian boreal forest, subarctic, and Arctic. Quat Sci Rev 23:1901–1924. https://doi.org/10.1016/j.quascirev.2004.03.013
Kessler TJ, Harvey CF (2001) Global flux of carbon dioxide into groundwater. Geophys Res Lett 28:279–282. https://doi.org/10.1029/2000GL011505

Kokelj SV, Burn CR (2003) Ground ice and soluble cations in near-surface permafrost, Inuvik, Northwest Territories, Canada. Permafr Periglac Process 14:275–289. https://doi.org/10.1002/ppp.458

Kokelj SV, Jorgenson MT (2013) Advances in thermokarst research. Permafr Periglac Process 24:108–119. https://doi.org/10.1002/ppp.1779

Kurylyk BL, Hayashi M, Quinton WL, McKenzie JM, Voss CI (2016) Influence of vertical and lateral heat transfer on permafrost thaw, peatland landscape transition, and groundwater flow. Water Resour Res 52:1286–1305. https://doi.org/10.1002/2015wr018057

Lacelle D, Vasil'chuk YK (2013) Recent progress (2007–2012) in permafrost isotope geochemistry. Permafr Periglac Process 24:138–145. https://doi.org/10.1002/ppp.1768

Lemieux J-M, Fortier R, Talbot-Poulin M-C, Molson J, Therrien R, Ouellet M, Banville D, Cochand M, Murray R (2016) Groundwater occurrence in cold environments: examples from Nunavik, Canada. Hydrogeol J 24:1497–1513. https://doi.org/10.1007/s10040-016-1411-1

Lemieux J-M, Fortier R, Murray R, Dagenais S, Cochand M, Delottier H, Therrien R, Molson J, Pryet A, Parhizkar M (2020) Groundwater dynamics within a watershed in the discontinuous permafrost zone near Umiujaq (Nunavik, Canada). Hydrogeol J https://doi.org/10.1007/s10040-020-02110-4

Ma R, Sun ZY, Hu YL, Chang QX, Wang S, Xing WL, Ge MY (2017) Hydrological connectivity from glaciers to rivers in the Qinghai-Tibet plateau: roles of suprapermafrost and subpermafrost groundwater. Hydrol Earth Syst Sci 21:4803–4823. https://doi.org/10.5194/hess-21-4803-2017

McKenzie JM, Voss CI (2013) Permafrost thaw in a nested groundwater-flow system. Hydrogeol J 21:299–316. https://doi.org/10.1007/s10040-012-0942-3

Messier V, Levesque B, Proulx J, Ward B, Libman M, Couillard M, Martin D, Hubert B (2007) Zoonotic diseases, drinking water and gastroenteritis in Nunavik: a brief portrait. Government of Quebec, Ministry of Communications, Quebec, QC

Michel FA (1986) Hydrogeology of the Central Mackenzie Valley. J Hydrol 85:379–405. https://doi.org/10.1016/0022-1694(86)90068-5

Michelsen N, van Geldern R, Roßmann Y, Bauer I, Schulz S, Barth JAC, Schüth C (2018) Comparison of precipitation collectors used in isotope hydrology. Chem Geol 488:171–179. https://doi.org/10.1016/j.chemgeo.2018.04.032

Moore R (2004) Introduction to salt dilution gauging for streamflow measurement: part 1. Streamline Watershed Manag Bull 7:20–23

Narancic B, Wolfe BB, Pienitz R, Meyer H, Lamhonwah D (2017) Landscape-gradient assessment of thermokarst lake hydrology using water isotope tracers. J Hydrol 545:327–338. https://doi.org/10.1016/j.jhydrol.2016.11.028

Parkhurst DL, Appelo C (2014) Description of input and examples for PHREEQC version 3–A computer program for speciation, batch-reaction, one-dimensional transport, and inverse geochemical calculations. US Geological Survey, Reston, VA

Piper AM (1944) A graphic procedure in the geochemical interpretation of water-analyses. Eos 25:914–923. https://doi.org/10.1029/TR025i006p00914

Provencher-Nolet L (2014) Détection de changement à court terme de la toundra arbustive à partir de photographies aériennes, région d'Umiujaq, Nunavik, Québec, Canada [Detection of short-term shrub tundra change from aerial photographs, Umiujaq area, Nunavik, Quebec, Canada]. Université du Québec, Institut national de la recherche scientifique (INRS), Quebec City, QC, Canada

Puls RW, Barcelona MJ (1996) Low-flow (minimal drawdown) groundwater sampling procedures. US EPA, Office of Research and Development, Office of Solid Waste and Emergency Response, Washington, DC

Romanovsky VE, Smith SL, Christiansen HH (2010) Permafrost thermal state in the polar northern hemisphere during the international polar year 2007–2009: a synthesis. Permafr Periglac Process 21:106–116. https://doi.org/10.1002/ppp.689

Rowland JC, Coon ET (2016) From documentation to prediction: raising the bar for thermokarst research. Hydrogeol J 24:645–648. https://doi.org/10.1007/s10040-015-1331-5

Rozanski K, Araguás-Araguás L, Gonfiantini R (1993) Isotopic patterns in modern global precipitation. In: Climate change in continental isotopic records. Geophys Monograph Ser 78, AGU, Washington, DC, pp 1–36

Schuster PF, Schaefer KM, Aiken GR, Antweiler RC, Dewild JF, Gryziec JD, Gusmeroli A, Hugelius G, Jafarov E, Krabbenhoft DP, Liu L, Herman-Mercer N, Mu CC, Roth DA, Schaefer T, Striegl RG, Wickland KP, Zhang TJ (2018) Permafrost stores a globally significant amount of mercury. Geophys Res Lett 45:1463–1471. https://doi.org/10.1002/2017gl075571

St-Jean G (2003) Automated quantitative and isotopic (13C) analysis of dissolved inorganic carbon and dissolved organic carbon in continuous-flow using a total organic carbon analyser. Rapid Commun Mass Spectrom 17:419–428. https://doi.org/10.1002/rcm.926

Stiff HA (1951) The interpretation of chemical water analysis by means of patterns. J Petroleum Technol 192:376–378. https://doi.org/10.2118/951376-G

Stocker T (2014) Climate change 2013: the physical science basis: Working Group I contribution to the Fifth assessment report of the Intergovernmental Panel on Climate Change, Cambridge University Press, New York

Stotler RL, Frape SK, Ruskeeniemi T, Ahonen L, Onstott TC, Hobbs MY (2009) Hydrogeochemistry of groundwaters in and below the base of thick permafrost at Lupin, Nunavut, Canada. J Hydrol 373:80–95. https://doi.org/10.1016/j.jhydrol.2009.04.013

Stotler RL, Frape SK, Freifeld BM, Holden B, Onstott TC, Ruskeeniemi T, Chan E (2011) Hydrogeology, chemical and microbial activity measurement through deep permafrost. Ground Water 49:348–364. https://doi.org/10.1111/j.1745-6584.2010.00724.x

Truchon-Savard A, Payette S (2012) Black spruce colonization of forest-tundra snow patches of eastern Canada Paper presented at the 42nd International Arctic workshop, Winter Park, CO, March 2012

Utting N, Lauriol B, Mochnacz N, Aeschbach-Hertig W, Clark I (2013) Noble gas and isotope geochemistry in western Canadian Arctic watersheds: tracing groundwater recharge in permafrost terrain. Hydrogeol J 21:79–91. https://doi.org/10.1007/s10040-012-0913-8

van Geldern R, Barth JAC (2012) Optimization of instrument setup and post-run corrections for oxygen and hydrogen stable isotope measurements of water by isotope ratio infrared spectroscopy (IRIS). Limnol Oceanogr Methods 10:1024–1036. https://doi.org/10.4319/lom.2012.10.1024

van Geldern R, Verma MP, Carvalho MC, Grassa F, Delgado-Huertas A, Monvoisin G, Barth JA (2013) Stable carbon isotope analysis of dissolved inorganic carbon (DIC) and dissolved organic carbon (DOC) in natural waters: results from a worldwide proficiency test. Rapid Commun Mass Spectrom 27:2099–2107. https://doi.org/10.1002/rcm.6665

Vogel JC (1993) Variability of carbon isotope fractionation during photosynthesis. In: Hall AE, Farquhar GD (eds) Stable isotopes and plant carbon-water relations. Academic, San Diego, CA, pp 29–46

Walvoord MA, Kurylyk BL (2016) Hydrologic impacts of thawing permafrost: a review. Vadose Zone J 15:20. https://doi.org/10.2136/vzj2016.01.0010

Walvoord MA, Voss CI, Wellman TP (2012) Influence of permafrost distribution on groundwater flow in the context of climate-driven permafrost thaw: example from Yukon Flats Basin, Alaska, United States. Water Resour Res 48. https://doi.org/10.1029/2011WR011595

Wellman TP, Voss CI, Walvoord MA (2013) Impacts of climate, lake size, and supra- and sub-permafrost groundwater flow on lake-talik evolution, Yukon Flats, Alaska (USA). Hydrogeol J 21:281–298. https://doi.org/10.1007/s10040-012-0941-4

Williams JR (1970) Ground water in the permafrost regions of Alaska. US Government Printing Office, Washington, DC

Wolfe BB, Karst-Riddoch TL, Hall RI, Edwards TWD, English MC, Palmini R, McGowan S, Leavitt PR, Vardy SR (2007) Classification of hydrological regimes of northern floodplain basins (Peace-Athabasca Delta, Canada) from analysis of stable isotopes (delta O-18, delta H-2) and water chemistry. Hydrol Process 21: 151–168. https://doi.org/10.1002/hyp.6229

Woo M-K, Kane DL, Carey SK, Yang D (2008) Progress in permafrost hydrology in the new millennium. Permafr Periglac Process 19:237–254. https://doi.org/10.1002/ppp.613

Ye B, Yang D, Zhang Z, Kane DL (2009) Variation of hydrological regime with permafrost coverage over Lena Basin in Siberia. J Geophys Res Atmos 114. https://doi.org/10.1029/2008JD010537